Flame Heat Transfer and Concurrent Flame Spread in a Ceiling Fire

YUJI HASEMI and MASASHI YOSHIDA
Building Research Institute
Ministry of Construction
Tsukuba-City, Ibaraki, 305, Japan

YUTAKA YOKOBAYASHI* and TAKAO WAKAMATSU
School of Science & Engineering
Science University of Tokyo
Noda-City, Chiba, 278, Japan

ABSTRACT

Measurements of flame length, flame heat transfer and flame spread are made on one-dimensional horizontal ceiling confined with two water-cooled soffits parallel to the flow field. Correlations with heat release rate are derived for flame length and flame heat transfer. Sensitivity to external heating and pilot flame intensity is studied on flame spread. Applicability of linearized flame spread theory for ceiling fires is examined using the test data.
Key Words: ceiling fire, flame spread, flame length, heat transfer.

INTRODUCTION

Flame development under a ceiling is very often the direct trigger for the occurrence of flashover. In spite of the importance of ceiling fires for fire safety, there are few laboratory measurements of this phenomenon[1,2]. It is seldom that a room fire starts on ceiling, and different fire growth scenarios may precede the ignition on the ceiling surface. Fire source on the floor intense enough to ignite directly the ceiling, fire of a plain wall, and a fire in a wall corner are among the typical fire scenarios leading to a ceiling fire. Such differences of fire scenarios may influence the behavior of ceiling fire itself; horizontal flame under ceiling, the main driving force of the flame spread along the ceiling, may result from the interaction of ceiling fire and other burning objects by which the ceiling was ignited. For the prediction of ceiling fires in different fire scenarios, it is important to model a pure ceiling fire, i.e. flame spread beneath the ceiling starting from an ignition source on the ceiling, as the substantial process of fire growth beneath a ceiling in any scenario. This paper reports results of measurements of flame length, flame heat transfer and flame spread with fuel injection from the ceiling surface as a first approach to model ceiling fires. Correlations for flame length and heat transfer are the key for the analysis of concurrent flame spread as has been established for upward turbulent wall fires, another typical concurrent flame spread in fire[3 - 8].

*Present affiliation: Technical Research Institute, Sekisui House Co., Kyoto-fu, Japan.

A one dimensional line trench beneath a ceiling confined with parallel soffits was used for simplicity although circular flame development is commoner in real fires. Flame heat transfer correlations were derived from measurements of flame length and heat flux to the ceiling from steady flames due to a porous propane-fed line burner with the downward outlet flush to the noncombustible ceiling surface. This series of tests will be referred to as the steady flame tests. Correlation was first obtained between flame length and heat release rate and then between incident heat flux and the flame length. Flame spread tests were then conducted with medium density fiberboard(MDF), an industrial charring material, lined along the ceiling of the same trench apparatus. As a hot gas layer due to fire origin very often develops prior to the ignition to a combustible ceiling in real fires, influence of external heating on the flame spread was examined using electrical radiant panels for the external heating source.

EXPERIMENTAL ARRANGEMENT AND MEASUREMENTS

Figure 1 shows the experimental set up. The 2.73m x 0.91m noncombustible ceiling was composed of two layers of 12mm thick fiber reinforced cement(Perlite) boards. Two 0.10m wide 2.40m long water cooled copper plates were placed parallel to the flow field with 0.30m distance beneath the ceiling to maintain one dimensional flame flow. A 0.30m x 0.04m rectangular porous gas burner was placed as the fire source at an end of the trench confined by the soffits with its surface downward flush to the ceiling surface. In order to establish a one-dimensional flame spread from the burner surface, the outer side of the burner was further blocked with a 0.40 m deep Perlite soffit and the other end of the trench was left unconfined.

Steady Flame Tests

Measurements were made on the heat flux to the ceiling, fuel supply rate and flame length. Heat flux was monitored with Schmidt-Boelter heat flux gages with its surface flush to the ceiling. Flame length was monitored by video cameras; reported flame lengths are the average of the total flame length measured from the windward side of the burner observed by eye for at least 3 minutes with the interval of one second on video tape. In some tests a gas analysis was made in the exhaust duct to compare heat release rates estimated from fuel supply rate and by

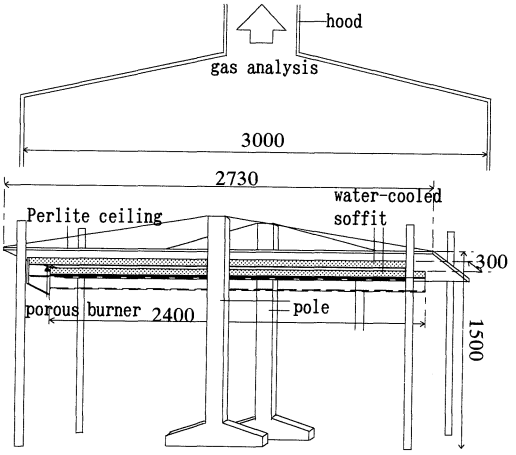

Figure 1 Experimental set up (dimensions in mm)

oxygen consumption method. Fuel supply rate to the burner was in the range approximately of 10 ℓ /min to 50 ℓ /min.

Flame Spread Tests

At each flame spread test, the trench part of the ceiling was lined with 10mm thick MDF. Surface temperature, flame length, and heat release rate were monitored with 0.1mm diameter chromel-alumel thermocouples, video cameras and gas analysis in the duct respectively. Surface heat flux was not measured as it had been anticipated that the holes through the specimen for heat flux gages could cause penetration of flame or hot gas through the specimen. Prevention of such penetration with noncombustible stopgap may also influence surface combustion of the specimen. MDF was selected as it had been used for upward flame spread tests already[9] and no dripping was anticipated during combustion. Each specimen was conditioned according to the ISO 525 before testing. Location of the pyrolysis front was identified by the jump in the time history of the surface temperature at each thermocouple[8]; 380℃ was chosen as the ignition temperature from the analysis of the test data(see Figure 5,6). Two 0.50m x 1.0m electrical radiant panels with 50kW/m^2 radiation capacity placed upward horizontally beneath the ceiling were used to simulate an external source to heat the ceiling surface, e.g. uniform heating by a smoke layer. The level of the external heat flux was chosen within the range of 0～10 kW/m^2. This range of incident heat flux had been reported in full scale room fire tests for temperature rise of the smoke layer not higher than 250K[10]. This smoke layer temperature range is believed as suitable to represent the early stage of a room fire where the ceiling fire is the main concern for fire safety assessment. Heat fluxes greater than this range resulted in flame spread too fast to observe visually. The radiant panels made a 2.0m long 0.5m wide radiation source, and were placed to cover the 2.0 m distance measured from the line burner out of the 2.4m long specimen. The heat flux to the ceiling trench just above the radiant panels was fairly uniform(within ±10%), however there was notable decay of heat flux beyond this distance. This condition should be considered in the interpretation of the test results. 17 tests were conducted, and three parameters, i.e. intensity of the ignition source, Q_B, external heat flux, qe", and initial condition of the surface temperature, Tb, were changed systematically. Tb is the surface temperature achieved by preheating with the radiant panels before ignition by the propane porous burner. The entire set-up was placed beneath a gas collection hood to measure heat release rate by the oxygen consumption method. ISO5657 Ignitability tests and heat release measurements with a Cone Calorimeter were conducted on the MDF to measure ignitability parameters and heat release rate in conditions close to the present tests[11].

FLAME LENGTH AND FLAME HEAT TRANSFER

Figure 2 summarizes the correlation between the flame length and heat release rate from the line burner per unit width assuming complete combustion. Flame length is nearly proportional to the heat release rate per unit width, $L_H \fallingdotseq 0.012 Q_\ell$, though $L_H = 0.02 Q_\ell^{0.9}$ leads to a slightly better fit. The nearly linear proportionality of flame length to heat release rate suggests a uniform entrainment to the ceiling flame. Interestingly this flame length is fairly close to that for a wall fire for around the similar range of heat release rate per unit width, $L_f \fallingdotseq 0.05 \sim 0.06 Q_\ell^{2/3}$[3, 12] although there is clear difference in the power dependence on heat release

rate. Results of the flame heat transfer measurements are summarized against the distance between heat flux gage and the windward edge of the burner,x, normalized by L_H in Figure 3. The test data were found to be highly concentrated along one single curve. The heat flux is nearly uniform for x below $0.4L_H$, and then decays with increasing distance as has been reported for wall fires[3,5]. However, the plateau heat flux, 20 kW/m^2, is weaker in the ceiling flames than in wall fires. The slope representing the decay for the ceiling trench is considerably less steep than for the wall fire correlation, and the heat flux can be represented as $q_c''= 6.36(x/L_H)^{-5/4}$. Heat flux beyond the flame, $x>L_H$, is thus larger in one-dimensional ceiling fires than in wall fires,while heat flux for $x<0.6L_H$ is generally greater in wall fires than in ceiling fires. Heat release rate obtained by the oxygen consumption method was only approximately 60% of the heat release assuming the complete combustion. Use of methane with the identical arrangement did not raise this value significantly, although a calibration with an unconfined upward porous methane burner under the identical hood showed over 92% combustion efficiency. It suggests notably low combustion efficiency in a ceiling fire even if the atmosphere is not vitiated. The flame length formula with net heat release rate is given by $L_H=0.023Q_\ell$; however, the test data are more scattered around this line than in Figure 2.

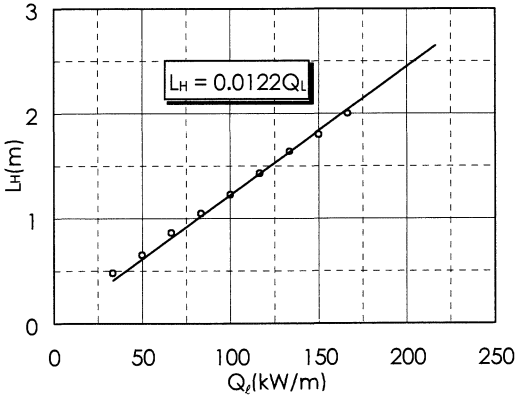

Figure 2 Relation between flame length and heat release rate per unit width(propane burner)

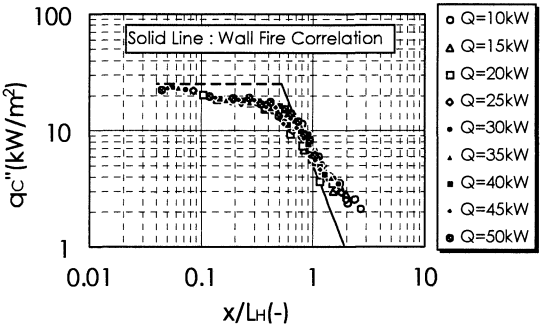

Figure 3 Flame heat flux vs. distance from the windward edge of fuel surface normalized by flame length

The flame length and heat transfer correlations thus obtained suggest the following general prospects for further analysis and safety assessment of flame spread in a ceiling configuration:
(1)Applicability of the linearized flame length approximation to ceiling fires
The proportionality of flame length to heat release rate per unit width suggests applicability of a flame spread theory with linearized flame length approximation such as the SQW equation[4]. It may simplify further analysis and evaluation of ceiling fires.
(2)Weaker flame spread beneath combustible ceiling than on wall
The weaker heat flux within the flame in the present test than in wall fires suggests a weaker flame spread beneath a ceiling than on a wall if the surface is not exposed to any external heating source. This prospect is hardly consistent with experience with real fires and large scale burn tests which generally suggests ceiling fires more dramatic than wall fires. The smoke layer preheating the whole ceiling surface with the heat generated by the ceiling fire itself can be a driving force for the spread of a ceiling fire, and may resolve this difference.

FLAME SPREAD BENEATH CEILING

Table 1 is a summary of the conditions and results of the flame spread tests conducted on MDF. x_{po} is the initial condition of the pyrolysis zone length and was defined as $0.4L_H$, the area in which incident heat flux from the line burner is nearly uniform; this part was assumed to be ignited simultaneously in the analysis. x_{poff} was determined from the ultimate burn pattern and was defined as the maximum distance of the charred surface with crack. Figure 4 are examples of the ultimate burn patterns. The stagnant progress of charred surface near the sidewalls is probably because of the water cooling of the copper soffits. There was virtually no spread of flame beyond the flame front due to the ignition burner at test no.1.

Figure 5 is a summary of the time-history of the location of the flame front and estimated pyrolysis front, and heat release rate per unit width for the test no.10. In this presentation, it is assumed that arrival of the pyrolysis front is indicated by the surface temperature arriving the ignition temperature of MDF, 380℃, although ignition temperature and the surface temperature at the arrival of pyrolysis front may depend weakly on configuration and boundary conditions[2, 8]. The reported flame lengths during growing fires are the ultimate location of the flame tips on video tape at each time step; this definition should lead to a longer flame length than the time-averages in the steady flame tests. Heat release from the line burner was removed from this presentation. Average flame length from the pilot burner was approximately 0.40m. Heat release rate is nearly proportional to the estimated distance of the pyrolysis front.

Figure 6 is a similar summary for test no.15. Curves for flame front, estimated pyrolysis front and heat release rate are considerably steeper than those for test no.10. Although flame spread was fast and the flame front finally overflew the specimen, the pyrolysis front seemed to stay enough shorter than the total length of the specimen, and progress of the pyrolysis front stopped rather suddenly. At both tests no.10 and no.15, heat release rate stopped growing at around the time when the pyrolysis front reached the maximum or slightly before that time. The stop of the heat release growth is attributed to the char formation. Proportionality of the flame length to heat release rate was confirmed at virtually all the tests so far conducted. In most of the tests ,time between the arrival of flame front and that of pyrolysis front, t^*, became nearly constant once the flame front became larger than the length of pilot flame until heat release rate was stagnated.

Table 1 Flame Spread Tests(Medium Density Fiberboard), Conditions and Summary Results

Test No.	External Heat Flux qe"(kW/m^2)	Initial Surface Temperature Tb(C)	Line Burner Heat Output QB(kW)***	xpo (m)	xpoff (m)	xpoff/xpo (-)	Maximum Heat Release Rate (kW/m)***
1	0	22.0	8.4(15)	0.26	0.6	2.61	15.0
4*	6.56	157.5	7.3(10)	0.24	1.12	4.65	75.9
5	5.59	187.9	7.3(10)	0.24	1.40	5.81	106.6
6	5.42	155.5	7.3(10)	0.24	1.00	4.17	67.8
7	5.38	129.2	7.3(10)	0.24	0.99	4.13	60.9
8	5.38	121.5	10.8(15)	0.33	1.33	4.01	82.8
9	5.38	125.4	13.80(20)	0.43	1.54	3.56	83.1
10	3.94	120.8	7.3(10)	0.24	0.98	4.06	55.3
11	6.60	183.6	7.3(10)	0.24	1.40	5.84	102.0
12	5.37	123.3	10.8(15)	0.33	1.26	3.79	73.7
13	5.41	151.3	7.3(10)	0.24	1.11	4.64	63.0
14	5.37	123.3	10.8(15)	0.33	1.41	4.25	65.0
15	6.66	204.5	7.3(10)	0.24	1.67	6.97	105.0
16	6.61	185.3	4.3(5)	0.17	1.45	8.65	99.0
17	9.13	329.5	4.3(5)	0.17	1.93**	11.49	200.7
18	3.99	139	7.3(10)	0.24	0.88	3.66	45.0
19	8.76	207	4.3(5)	0.17	1.74	10.36	104.3

* Test no.2 and 3 were conducted with other materials.

** External heat flux for x>2.0m was obviously weaker than the figure for qe" in the table. Cease of flame spread at around this distance could be due to this weaker heat flux.

*** The numbers outside the parentheses were measured with oxygen consumption method and those in the parentheses are based on the assumption of complete combustion.

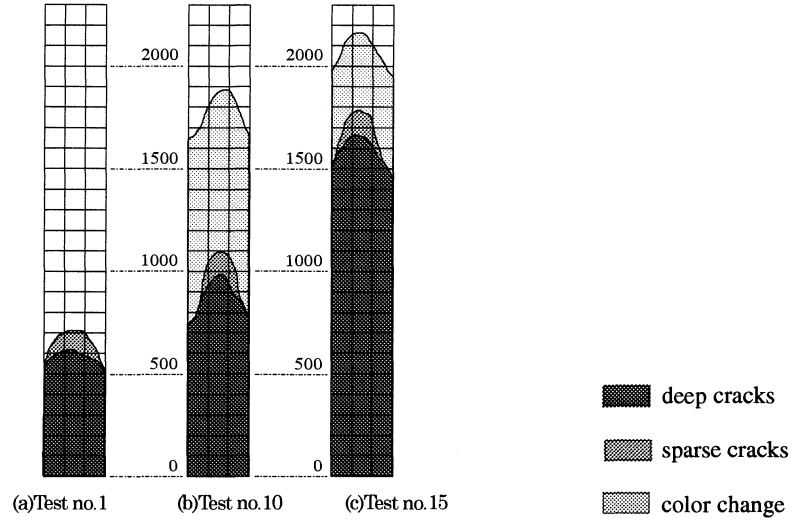

Figure 4 Ultimate burn patterns of the flame spread tests

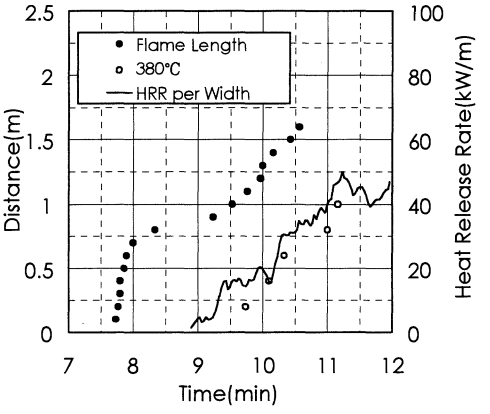

Figure 5 Flame front, estimated pyrolysis front, and heat release rate per unit width(test no.10)
Time was counted from the start of the preheating.

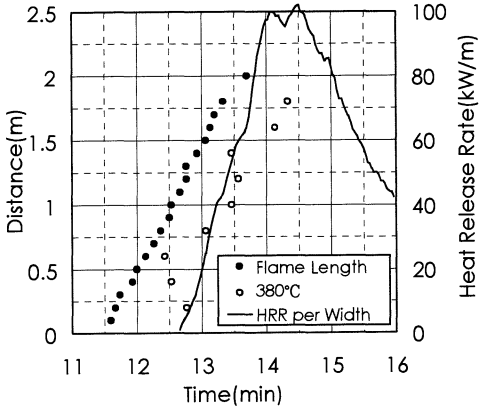

Figure 6 Flame front, estimated pyrolysis front, and heat release rate per unit width(test no.15)
Time was counted from the start of the preheating.

Sensitivity of Flame Spread to Test Parameters

The test results in Table 1 cover a notably wide range of x_{poff}/x_{po} value. According to the flame spread models based on linearized flame length approximation, x_{poff}/x_{po} value is considered as a function only of local heat release rate and ignitability of the material under the test condition, and is regarded as independent of the size of ignition source[6, 7, 9]. Comparing the data from the tests with different Q_B and similar q_e'' and T_b, e.g. among the tests no.7, 8 and 9 ,or between the tests no.12 and 14, the x_{poff}/x_{po} value is found not to be very sensitive to x_{po} or Q_B. Among the three test parameters, i.e. Q_B, q_e'' and T_b, x_{poff}/x_{po} value is primarily sensitive to T_b. Figure 7 is a summary of relation between x_{poff}/x_{po} and T_b. Although data from different external heat flux levels were collected together, most of the data are nearly on one curve where x_{poff}/x_{po} increases with T_b and jumps at around 200℃. As noted in the Table 1, the x_{poff}/x_{po} value for T_b =329.5℃ could have been greater if the heat flux to the specimen had been more uniform. Figure 8 shows heat release rates per unit width for different external heat flux levels ignited at identical surface temperature. Although the external heat fluxes are

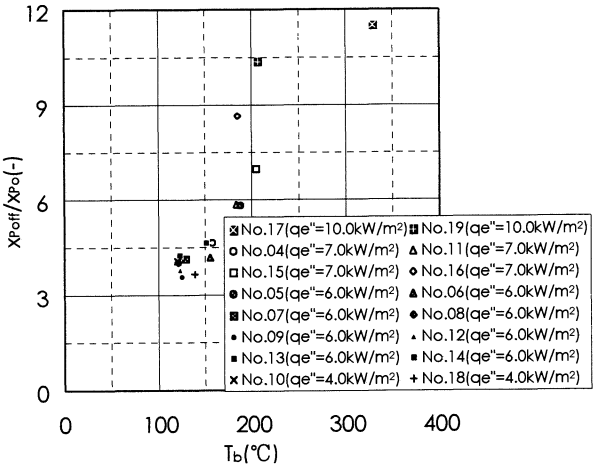

Figure 7 Relation between xpoff/xpo and external heat flux level

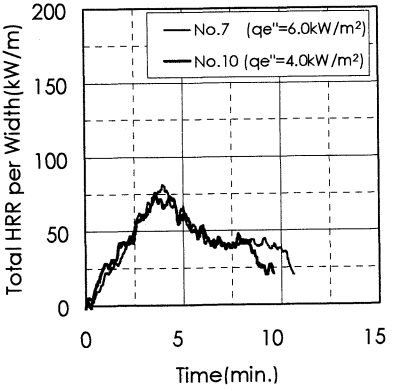

Figure 8 Heat release rate per unit width during flame spread tests (Tb=120℃)

different, the time history of heat release rate is nearly identical between these two conditions. These suggest primary importance of the temperature of ceiling at its sustained ignition for the growth of a ceiling fire.

According to the previous analyses on concurrent flame spread[14, 15, 16], external heating is believed to accelerate flame spread through two different mechanisms, augmentation of heat release rate from the pyrolysis zone and preheating of the unburnt surface. The primary dependence of flame spread velocity on the initial surface temperature in the present test demonstrates importance of the second mechanism for the development of ceiling fires.

Characteristic Time for Flame Spread and Characteristic Preheat Intensity

For the application of the linearized flame length approximation to the modeling of flame spread, it is necessary to use dynamic local heat release rate and characteristic time to ignition[6, 7]. These parameters can be basically obtained from the ISO 5657 Ignitability test and a dynamic heat release measurement such as the Cone Calorimeter test. One of the main

questions in the use of these bench scale tests is the heating condition to be used at the tests. In order to seek this condition for ceiling fires, comparison has been made between t* and the time to ignition at different heat flux levels obtained from the ISO 5657 Ignitability test. According to the thermal modeling of surface ignition of a combustible solid, square root of the time to ignition under a constant radiation is nearly inversely proportional to the heat flux and can be approximated by

$$t_{ig}^{-1/2} \fallingdotseq 1.18\{ \varepsilon q_e''/(k\rho c)^{1/2}(T_{ig} - T_o) - h/(k\rho c)^{1/2}\} \quad (1)$$

Since heat flux from ceiling flame to the ceiling surface is not always constant, characteristic preheat intensity, q_{er}'' is defined as the heat flux level in an ignitability test at which the time to ignition is equivalent to t* observed in the flame spread test. Practically q_{er}'' can be obtained by solving equation(1) for q_e'' with t* and Tb substituted into t_{ig} and To respectively. T_{ig} of MDF was assumed as 380℃, and $(k\rho c)^{1/2}/\varepsilon$ and $(k\rho c)^{1/2}/h$ were determined from the ignitability tests as 0.90 $kWs^{1/2}/m^2K$ and 428 $s^{1/2}$ respectively. Figure 9 is a summary of the relation between q_e'' and q_{er}'' thus obtained. q_{er}'' data scatter around 20kW/m^2 without strong dependency on q_e'' or Tb.

Comparison between Experimental and Theoretical x_{poff}/x_{po}

In order to evaluate validity of the Volterra type integral equation for concurrent flame spread, SQW equation[4], for ceiling fires, x_{poff}/x_{po} is compared between the present tests and calculation. Comparison is made in the Baroudi-Kokkala diagram[7] in which the asymptotic behavior of the solution of the SQW equation and x_{poff}/x_{po} are represented as a function of $a \equiv K \cdot q_o$, λ and τ where q_o and λ characterize local heat release rate by $q''(t)=q_o \cdot \exp(-\lambda t)$ and τ is a characteristic time for flame spread defined as $V_p=(x_f - x_p)/\tau$. τ is equivalent with

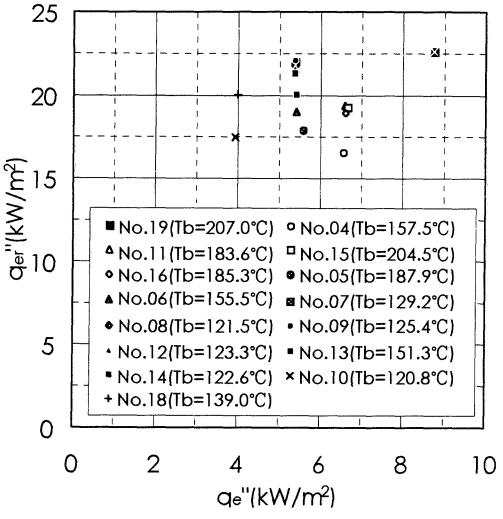

Figure 9 Relation between external heat flux level and characteristic preheat intensity, q_{er}''

t* at a steady-state flame spread[9]. qo and λ are estimated from the heat release rate of MDF measured with an intermediate scale calorimeter with vertical electrical radiant panels[11]. The intermediate scale heat release measurement was made at heat flux levels close to the present tests, 4kW/m^2, 6kW/m^2 and 8kW/m^2. Time to ignition at qe"=qer"=20kW/m^{2}with initial surface temperature To=Tb calculated from equation(1) was substituted into $\tau \cdot \lambda \bullet \tau$ and α values thus obtained for each test condition are mapped on the Baroudi-Kokkala diagram in Figure 10.

Experimental xpoff/xpo value from each test is also shown on the diagram. It is noteworthy that the experimental xpoff/xpo value is fairly close to the calculation represented by contours in Figure 10 for xpoff/xpo not larger than 5, while the calculation seems to lead to overestimate of xpoff/xpo for larger xpoff/xpo. This agreement between experiment and calculation for small xpoff/xpo and the discrepancy for large xpoff/xpo is probably because of the constant t* assumed for the characteristic preheat intensity. From the nature of the solution of the SQW equation, this assumption should be valid only in the vicinity of the straight line represented by α =0, and below this line t* is believed to be shorter than τ [6, 9]. Since the time to ignition at the characteristic preheat intensity, tigr, is essentially equivalent with t*, substitution of tigr into τ in the Baroudi-Kokkala diagram should result in the overestimate of xpoff/xpo in the domain beneath the α =0 straight line.

CONCLUSIONS

Measurements of flame heat transfer and flame spread beneath ceiling have been conducted using a one-dimensional ceiling trench with water-cooled side walls. Following conclusions can be drawn on flames and flame spread in a one-dimensional ceiling fire configuration.

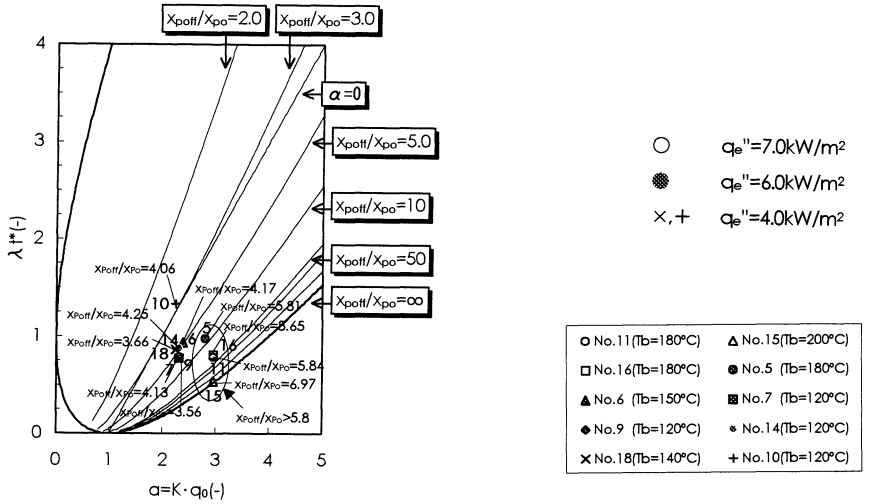

Figure 10 Comparison of experimental xpoff/xpo and theoretical xpoff/xpo based on the SQW equation(tigr: time to ignition at the *characteristic preheat intensity*)

(1)Length of a one-dimensional ceiling flame is nearly proportional to heat release rate.
(2)Incident heat flux from ceiling flame to the ceiling surface is represented as a function of distance normalized by flame length.
(3)No flame spread beyond pilot flame can be observed for MDF in a ceiling trench configuration without external heating.
(4)One dimensional flame spread along a MDF ceiling is sensitive to the initial ceiling surface temperature and is insensitive to the intensity of pilot flame.
(5)Preheat by flame between flame front and pyrolysis front of a ceiling fire is nearly equivalent with constant heating of 20kW/m^2 for the time from the arrival of flame front to that of pyrolysis front.
(6)xpoff/xpo estimated from the Baroudi-Kokkala diagram with material properties obtained from heat release and ignitability tests is close to experiment for xpoff/xpo not larger than 5.

ACKNOWLEDGMENT

The authors wish to thank Messrs. R.Takaike, A. Inoue, A. Takakuwa, and Y.Wakabayashi, students of the Department of Architecture and Architectural Engineering, School of Science and Engineering, Science University of Tokyo, for the assistance in the present experiments.

TERMINOLOGY

K : flame length to heat release rate ratio[m/(kW/m), K=0.012 for the present study]
L_f : flame height[m]
L_H : horizontal flame length beneath ceiling[m]
Q_B : heat release rate from ignition burner[kW]
Q_ℓ : heat release rate per unit width[kW/m]
Tb : surface temperature of combustible ceiling at the ignition to the ignition burner[℃]
T_{ig} : ignition temperature[℃]
To : ambient temperature, or initial surface temperature in equation(1)[℃]
V_p : flame spreading velocity[m/s]
a : flame length for the peak heat release rate per unit area(K•qo")[-]
c : specific heat[kJ/kgK]
h : surface heat transfer coefficient[kW/m^{2}K]
k : thermal conductivity[kW/mK]
q"(t) : heat release rate per unit area[kW/m^2]
qc" : flame heat flux in ceiling configuration[kW/m^2]
qe" : external heat flux[kW/m^2]
qer" : characteristic preheat intensity[kW/m^2]
qo" : peak heat release rate per unit area[kW/m^2]
t : time[s]
t* : time from the arrival of flame front to that of pyrolysis front in concurrent flame spread[s]
t_{ig} : time to ignition[s]
t_{igr} : time to ignition at the characteristic preheat intensity[s]
x : leeward distance from the upstream side of ignition burner[m]
xf : location of flame front[m]
xp : location of pyrolysis front[m]
xpo : initial condition of the length of pyrolysis zone which is ignited simultaneously by the

pilot flame[m]

xpoff : length of the maximum pyrolysis front[m]

α : parameter controlling stability of flame spread

ε : emissivity[-]

λ : constant representing decay of local heat release[1/s]

ρ : density[kg/m^3]

τ : characteristic time for flame spread[s]

REFERENCES

1. Ohtani, H., Miyazawa, S., and Nakaya, I.: Experimental Study on Bottom Surface Combustion of Wood, Annual Meeting, Japan Association for Fire Science and Engineering, 1990(in Japanese).
2. Atreya, A.: Private Communication, 1991.
3. Hasemi,Y.: Thermal Modeling of Upward Flame Spread, Proceedings of the First International Symposium on Fire Safety Science, Gaithersburg, 1985.
4. Saito,K., Quintiere,J.G., and Williams,F.A.: Upward Turbulent Flame Spread, Proceedings of the First International Symposium on Fire Safety Science, Gaithersburg, 1985.
5. Quintiere, J.G., Harkleroad, M. and Hasemi,Y.: Wall Flames and Implications for Upward Flame Spread, Combustion Science and Technology, Vol.48, No.1, 1986.
6. Thomas,P.H., and Karlsson,B.: On Upward Flame Spread, Department of Fire Safety Engineering, Lund University, 1991.
7. Baroudi,D., and Kokkala,M.: Analysis of Upward Flame Spread, VTT Publications 89, 1992.
8. Atreya,A., Carpentier,C., and Harkleroad,M.: Effect of Sample Orientation on Piloted Ignition and Flame Spread, Proceedings of the First International Symposium on Fire Safety Science, Gaithersburg, 1985.
9. Hasemi,Y., Yoshida,M., Yasui,N., and Parker,W.J.: Upward Flame Spread along a Vertical Solid for Transient Local Heat Release Rate, Proceedings of the Fourth International Symposium on Fire Safety Science, Ottawa, 1994.
10. Hasemi,Y., Yoshida,M., Nakabayashi,T., and Yasui,N.: Transition from Room Corner Fire to Flashover in a Compartment with Combustible Walls and Noncombustible Ceiling, Proceedings of the First ASIAN Conference on Fire Science and Technology, Hefei, 1992.
11. Hasemi,Y., Yoshida,M., Kikuchi,R., Yamamoto,E., and Takaike,R.: Heat Release Rates Measured by the Cone Calorimeter and Intermediate Scale Electrical Radiant Panels, The 13th Joint Meeting, UJNR on Fire Research and Safety, Gaithersburg, 1996.
12. Delichatsios,M.A.: Modeling of aircraft cabin fires, FMRC Technical Report 1984.
13. Karlsson,B.: Modeling Fire Growth on Combustible Lining Materials in Enclosures, Lund University, Department of Fire Safety Engineering, Report TVBB-1009, 1992.
14. Fernandez-Pello,A.C.: Upward Laminar Flame Spread under the Influence of Externally Applied Thermal Radiation, Combustion and Flame, 17, 1977.
15. Hasemi,Y., Yoshida,M., Nohara,A., and Nakabayashi,T.: Unsteady-state Upward Flame Spreading Velocity along Vertical Combustible Solid and Influence of External Radiation on the Flame Spread, Proceedings of the Third International Symposium on Fire Safety Science, Edinburgh, 1991.
16. Delichatsios, M.M., Wu, P., Delichatsios,M.A., Lougheed,G.D., Crampton, G.P., Qian,C., Ishida,H., and Saito,K.: Effect of External Radiant Heat Flux on Upward Fire Spread: Measurements on Plywood and Numerical Predictions, Proceedings of the Fourth International Symposium on Fire Safety Science, Ottawa, 1994.